Critical lines and massive phases in quantum spin ladders with dimerization

J. Almeida,[1] M. A. Martin-Delgado,[1] and G. Sierra[2]
[1]*Departamento de Física Teórica I, Universidad Complutense, 28040 Madrid, Spain*
[2]*Instituto de Física Teórica, CSIC–UAM, Madrid, Spain*
(Received 30 July 2007; revised manuscript received 31 October 2007; published 17 March 2008)

We determine the existence of critical lines in dimerized quantum spin ladders in their phase diagram of coupling constants using the finite-size density matrix renormalization group algorithm. We consider both staggered and columnar dimerization patterns, and antiferromagnetic and ferromagnetic interleg couplings. The existence of critical phases depends on the precise combination of these patterns. The nature of the massive phases separating the critical lines are characterized with generalized string order parameters that determine their valence-bond-solid content.

DOI: 10.1103/PhysRevB.77.094415 PACS number(s): 75.10.Jm, 74.20.Mn

I. INTRODUCTION

The issue of the existence of massive or critical phases in quantum spin systems has motivated a great deal of study in strongly correlated systems since the seminal work on the Haldane conjecture.[1] This issue became a central problem when more complicated arrays of spins chains, known as quantum spin ladders, were discovered experimentally in cuprate materials that exhibit high-T_c superconductivity when they are appropriately doped.[2,3]

From a more fundamental viewpoint, the study of critical and massive phases in quantum spin ladders offers the possibility of a testing ground for studying complicated quantum many-body effects, which, in some instances, underly the physics of unconventional phases of matter.[4] A variety of spin ladders with different numbers of legs have been synthesized based on cuprate materials, such as $SrCu_2O_3$, $Sr_2Cu_3O_5$, etc.,[5,6] or in other families of compounds $La_{4+4n}Cu_{8+2n}O_{14+8n}$,[7] and they present typically antiferromagnetic rung couplings among the legs of the spin ladders. It is also possible to find materials with less conventional ferromagnetic rung couplings like in certain chemical compounds such as PNNNO and PIMNO.[8] In addition, the new tools to study strongly correlated systems based on optical lattices open the possibility of implementing a variety of quantum spin systems including ladders.[9,10]

The phase diagram of quantum spin ladders with staggered dimerization was conjectured on the basis of analytical nonperturbative methods[11] like the nonlinear sigma model (NLSM) complemented with additional information from the weak and strong coupling limits in the rung coupling constants and dimerization parameters. Later, a series of different approximate analytical studies[12,13] has been favorable for the existence of a critical line in the simplest case of a two-leg spin ladder with staggered dimerization. Also, some preliminary numerical methods with the Lanczos algorithm[14,15] have shown support for this fact for ladders with a small size. Despite these several studies, a complete nonperturbative numerical analysis of these staggered low dimensional quantum spin systems have remained as an open problem.

In this paper, we study a three-leg quantum spin ladder with different types of rung couplings (either antiferromagnetic or ferromagnetic) and different dimerization patterns. These ladders are complex enough so as to serve as paradigmatic examples for testing the conjectured phase diagrams.[11] In order to achieve a conclusive answer to the conjectured phase diagrams for this system, we resort to a nonperturbative numerical tool like the density matrix renormalization group (DMRG) method.[16–20] In particular, we employ its finite-size version based on the sweeping procedure to improve the convergence of the iterative steps. The characterization of the different phases separated by the critical lines is performed with a DMRG calculation of generalized string order parameters (SOPs)[21] that were introduced to distinguish between massive phases in dimerized spin chains[22] even when the localized spins in the chain take on half-integer values. These SOPs are extensions of the originally nonlocal vacuum-expectation values introduced for integer spins and the like.[23,24]

The elucidation of the existence of a critical line in the phase diagram of quantum spin ladders with staggered dimerization is not straightforward when the ladders have end points as in the open boundary conditions geometry demanded by the standard DMRG method. Thus, we have to resort to the numerical analysis of the low-lying spectrum of excitations in order to extract the correct gap in the bulk of the system when studying the universal properties of these ladders in the thermodynamic limit (length going to infinity).[25]

The string order parameter is a theoretical construct in a condensed matter that allows the characterization of massive phases with a valence bond solid (VBS) structure. It has never been measured experimentally. However, with the engineering of optical lattices, it would be possible to address a direct measurement of this important quantity.[10]

Next, we summarize the main results of this paper.

(1) We have computed accurately the critical lines of the phase diagram of a dimerized (staggered) three-leg ladder in the antiferromagnetic regime $J'>0$ by means of the DMRG algorithm. In this regard, it is important to notice that the existence of the mentioned critical lines has only been conjectured previously based on analytical methods such as the NLSM.[11]

(2) We also prove the existence of critical lines in the case of the dimerized (columnar) three-leg ladder with ferromagnetic couplings $J'<0$ between legs and obtain accurately its

shape. In these systems, no NLSM studies have been carried out.

(3) In both types of ladders, based on our DMRG calculations, we provide numerical fits for the shape of the critical lines, something that is out of reach of NLSM methods since these are only trustable in the strong coupling region $J' \gg J$.

(4) We have uncovered the nature of the quantum phases separated by the critical lines and rigorously characterized them. To achieve this task, we make use of a generalized order parameter (SOP) which, interestingly enough, allows us to recast our results in terms of the VBS picture in both types of ladders. We remark that it was not obvious that the ground state of these systems indeed had a VBS nature, and it cannot be easily guessed beforehand without measuring the SOP. We also stress the importance of the success in characterizing the VBS types in systems not strictly one dimensional like dimerized ladders.

The paper is organized as follows: In Sec. II, we introduce the two patterns of dimerization in three-leg ladders. One is columnar (1) with ferromagnetic rung couplings, while the other is alternating (2) with antiferromagnetic rung couplings. In the former, we establish a helpful connection with the $S=\frac{3}{2}$ antiferromagnetic alternating chain in a certain strong coupling limit. We recall several conjectures about the phase diagram of both three-leg Heisenberg models[11] that motivate their study with DMRG in order to clarify them. In Sec. III, we perform the DMRG calculations of the low-energy gaps in both models of three-leg ladders as a function of the various coupling constants. With this information, we can establish the phase diagram, and thus, we establish the validity of the conjectured diagram.[11] In addition, we can give a precise location of the critical lines, and we find qualitative differences between these critical lines in each model. In Sec. IV, we introduce generalized string order parameter to characterize the nature of the massive phases separated by the critical lines found in the previous section. These string orders are measured with DMRG techniques, and we show that they are a valuable tool for detecting VBS states in dimerized quantum spin ladders with different patterns of dimerization. Section V is devoted to the conclusions. In the Appendix, we study with DMRG the $S=\frac{3}{2}$ alternating spin ladder and its generalized string order parameters. This case appears as a limiting case in the study of the ferromagnetic three-leg ladder with columnar dimerization, and it is used as a guiding example to find the phase diagram.

II. QUANTUM HAMILTONIANS FOR THREE-LEG SPIN LADDERS WITH DIMERIZATION

One of the main interests established in Ref. 11 was the existence of an interplay between three-leg ladders with a columnar dimerization pattern and ferromagnetic interleg, or rung, couplings on one side and three-leg ladders with alternating dimerization and antiferromagnetic rung couplings on the other. The point was that both arrangements of three-leg ladders should exhibit critical lines, while neither was their precise location known nor the nature of the massive phases they separated determined. This is the open problem that we address here by means of the DMRG method. To this end, we start introducing both arrays of ladders since they are the candidates to exhibit critical lines.

Thus, we are mainly interested in studying a possible connection between two different arrangements of spins $\frac{1}{2}$ forming a three-leg ladder, which interact via Heisenberg terms. Both of them combine bonds of different strengths parametrized by a constant γ and two different types of coupling constants, J for the Heisenberg interaction between spins along the legs, and J' for similar interactions between the rungs of the legs. Since the physics of the problem depends only on the ratio J'/J, the constant J will from now on be given a fixed antiferromagnetic value $J=1$. The other constant J' will have a positive sign in one of the models and a negative one in the other. In addition to this difference, both models will also differ in the staggering pattern as we shall discuss below.

We next describe the model corresponding to the region with $J'<0$, with the bond alternation pattern such that every one of the three legs begins with a strong bond followed by a weaker one; that is, the bond alternation follows a *columnar pattern*. The explicit Hamiltonian of this arrangement is

$$H_F = J \sum_{\ell=1,2,3} \sum_{i=1}^{L-1} [1-(-1)^i \gamma] \mathbf{S}_i(\ell) \cdot \mathbf{S}_{i+1}(\ell) + J' \sum_{i=1}^{L} \mathbf{S}_i(1) \cdot \mathbf{S}_i(2) + J' \sum_{i=1}^{L} \mathbf{S}_i(2) \cdot \mathbf{S}_i(3), \qquad (1)$$

where L denotes the longitudinal length of the three-leg ladder, $\mathbf{S}_i(\ell)$ is a spin-$\frac{1}{2}$ operator located at site i of the ℓth leg with $0<i\leqslant L$, and γ is the dimerization parameter that sets the relative strength of the bonds that interact with Heisenberg coupling constant J along the leg of the ladder and J' on the rungs of the legs.

Since the coupling among legs is ferromagnetic, we know that for values $|J'| \gg 1$, this model converges to an effective $S=3/2$ staggered spin chain. Studies with the NLσM method predicts[26] for this chain the existence of three critical points in the interval $\gamma \in [-1,1]$ placed at $\gamma_c = \pm 2/3$ and $\gamma_c = 0$. Numerical studies showed that, in fact, these points correspond to $\gamma = \pm 0.42$ and $\gamma = 0$.[27,28] Since the $S=3/2$ dimerized spin chain gives us valuable information about the expected massive phases of the ladder in the strong ferromagnetic regime, and since there exist some subtleties regarding the string order parameters that may lead to confusion, we have included a numerical study of this chain in the Appendix.

For the completely antiferromagnetic regime $J'>0$, we will use another staggering pattern that differs with respect to the previous one. In this case, only the first and third leg begin with a strong bond, while the second one begins with a weak one; that is, the bond alternation is not columnar anymore but still follows a regular pattern that is called *alternating*. The Hamiltonian of this model is

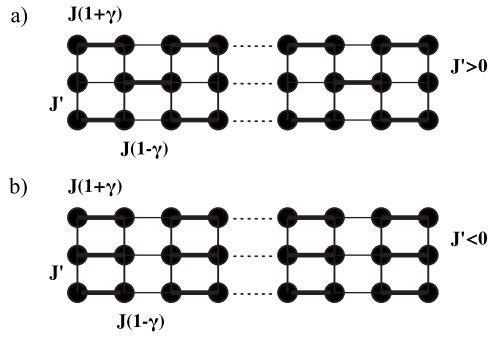

FIG. 1. Pictorial representation of the Hamiltonians corresponding to (a) the completely antiferromagnetic ($J'>0$) model (2) with alternated staggering and (b) the ferromagnetic ($J'<0$) model (1) with columnar staggering.

$$H_{\mathrm{AF}} = J \sum_{\ell=1,2,3} \sum_{i=1}^{L-1} [1 + (-1)^{i+\ell}\gamma]\mathbf{S}_i(\ell) \cdot \mathbf{S}_{i+1}(\ell) + J' \sum_{i=1}^{L} \mathbf{S}_i(1) \cdot \mathbf{S}_i(2) + J' \sum_{i=1}^{L} \mathbf{S}_i(2) \cdot \mathbf{S}_i(3), \qquad (2)$$

with the same conventions as before. A pictorial representation of this Hamiltonian, together with the Hamiltonian of the ferromagnetic model, is shown in Fig. 1.

With this arrangement, it is also possible to effectively and approximately map the model onto a NLσM, and again this formalism predicts a critical behavior in the phase diagram of the couplings J'/J vs. γ.[11] However, this behavior is only reliable in the strong coupling limit $J'/J \gg 1$. More specifically, it predicts a critical curve running from the point ($\gamma=2/3$, $J'=0$) to ($\gamma=1$, $J'=4/5$) and another one which is the mirror reflection of the latter with respect to the J' axis. These predictions, however, shall be considered only as qualitative approximations of the real behavior of the system. In this particular case, it is evident that the critical line must cut the γ axis exactly at $\gamma=0$ since that point corresponds to two decoupled $S=1/2$ staggered Heisenberg chains. However, this behavior is missed by the NLσM technique. On the other hand, this model has no apparent limits, which can give us a hint on the phases that arise. In Sec. III, however, our DMRG computations will give strong evidence of their nature.

Despite the differences in both models, i.e., different signs of J' and different staggering patterns, there are various features that connect them. First of all and more important is that, at least in the line $\gamma=0$, both models are constinuosly related as we vary $J'<0$ to $J'>0$. On the other hand, according to NLσM, the first model is critical only in the region $J'>0$, while the second one has only critical lines in the complementary part $J'<0$. This dual-like behavior, combined with the expectation that the ground state of both models is a valence bond solid, rouse the belief about the possibility of establishing a connection among their phase diagrams.[11] We shall see to what extent these expectations are fulfilled with the help of the DMRG technique and the generalized string order parameters.

III. GROUND STATE DEGENERACY AND EXISTENCE OF CRITICAL LINES

Massive quantum phases are characterized by an energy gap from the ground state (degenerate or not) to the first excited state. On the contrary, critical phases are characterized by a gapless spectrum between these energy levels. We have used the finite-size DMRG algorithm to compute the low-energy levels and, thus, the corresponding gaps in order to identify the gap in the bulk of the system when we send the length of the three-leg ladders to infinity (thermodynamic limit).

It is known that in the case of integer spin chains, some configurations of VBS states can break a hidden $Z_2 \times Z_2$ symmetry[21] that makes the ground state degenerate. This degeneration is a reflection of the spin-end effects in an antiferromagnetic Heisenberg chain of $S=1$ spins.[29] In systems other than the parent Hamiltonians of the VBS states, but close enough to this picture, and when using open boundary conditions, this degeneracy is typically approximate and the energy of the near-degenerate states decays exponentially with the size to a unique infinite volume ground state.

Figure 2 shows the energy differences between the ground state and the two first excited states in both models (1) and (2). We observe in this figure that Δ_{10} accounts for the degeneracy mentioned in the previous paragraph: In the completely antiferromagnetic model (2), the first excited state is clearly above the ground state in the phase corresponding to low values of γ, while it is degenerate in the rest of the γ interval. On the contrary, the ground state of the ferromagnetic model (1) is degenerate for low values of γ, while it has a finite gap in the rest. As for Δ_{20}, it corresponds, in fact, to the gap of the spectrum in the degenerate regions, while it clearly differs from the gap Δ_{10} in the nondegenerate regions. Finally, the energy difference Δ_{21} coincides in both regions and both models with the gap of the massive phases. This holds true up to slight deviations due to finite-size effects and irrespective of the degeneracy of the ground state, Thus, we may conclude that this gap Δ_{21}, is, in fact, the same one that survives when using periodic boundary conditions.

As mentioned in the previous section, the existence of critical lines (characterized by a gapless spectrum) in both models (1) and (2) is supported by arguments coming from the strong coupling limit in the case of model (1), and NLσM is valid in both of them. These arguments are, however, not conclusive. In this section, we will prove numerically that these lines exist, and we give an accurate estimation of its shape and location. To this end, we will find the critical values $\gamma_c(J')$ that make the gap $\Delta_{21}[\gamma_c(J')]$ vanish. It is very important at this point to emphasize that an exactly vanishing value of the gap shall only be attained in the thermodynamic limit. For finite-size systems, the magnitude of the gap remains finite and gets closer and closer to zero as we increase the size. In our case, however, critical points separate massive gapped phases; therefore, for large enough but still computationally feasible sizes, the gap at these points attain a local minimum value and can be accurately computed. In Fig. 3, we provide the gap Δ_{21} of the columnar ferromagnetic ladder for different sizes and an arbitrary choice of $J'=-4$. The existence of the mentioned minimum

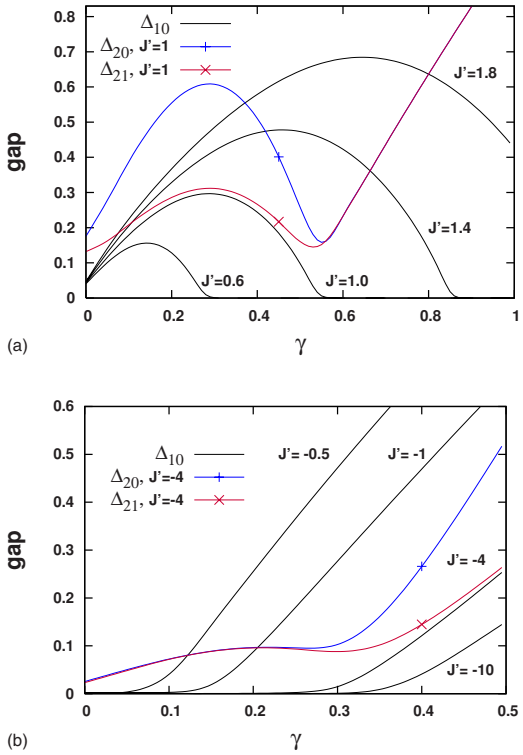

FIG. 2. (Color online) Energy gaps between the ground state and two first excited states: (a) in model (2) and (b) in model (1). For the sake of clarity, Δ_{20} and Δ_{21} are shown only for one value of J': (a) in $J'=1.0$ and (b) in $J'=-4$. It can be seen how the gap Δ_{21} indeed represents properly the gap of the spectrum irrespective of the degeneration of the ground state. The size of the ladders is $L=3\times 80$.

and how it tends toward zero can be observed as we increase the size. The scale of the figure may seem misguiding since it does not reflect the relative magnitude of the gap, which in the minimum of the $L=3\times 150$ curve is as low as a 0.01% of the ground state energy. An analogous tendency has been observed in the staggered antiferromagnetic case.

Figure 4 shows the critical region computed for both models (2) and (1). In order to compute these curves, we have used the finite DMRG algorithm in ladders of

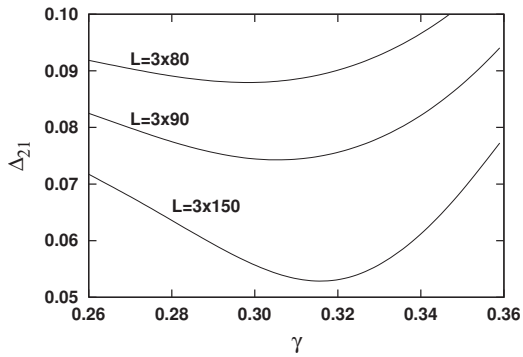

FIG. 3. Gap of the columnar ferromagnetic ladder for an arbitrary value $J'=-4$. The minimum value of the gap tends toward zero as we increase the size of the system and will eventually vanish in the thermodynamic limit.

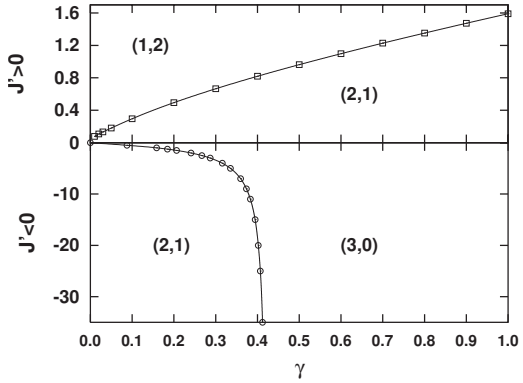

FIG. 4. Critical curves of model (1) with $J'>0$ and alternated staggering, and model (2) with $J'<0$ and columnar staggering. Each point in the critical lines has been obtained, keeping one parameter fixed and finding the value of the other parameter that minimizes the gap Δ_{21}. Computations have been performed on ladders of size $L=3\times 150$ retaining $m=400$ ($J'>0$ region) and $m=450$ ($J'<0$ region) states of the density matrix.

$L=3\times 150$ sites. For the completely antiferromagnetic model (2), we retained $m=400$ states of the density matrix and a Lanczos tolerance equal to 10^{-9}. The ferromagnetic model (1) turned out to be numerically more demmanding, and we set $m=450$ and the tolerance equal to 10^{-10}. Two sweeps of DMRG were enough in both models to make the energies converge. These results clearly confirm the conjectured phase diagrams for these three-leg models.[11]

The solid lines in Fig. 4 are only a guide for the eye. We have, however, used our numerical data to estimate the best fit to that critical lines. For the region $J'>0$, we have used a simple potential function of the form

$$J'_c = a\gamma_c^r. \tag{3}$$

The best value of each parameter has been obtained by performing a least squares fit and are equal to $a=1.59\pm 0.01$ and $r=0.72\pm 0.01$. As for the critical line in the semiplane $J'<0$, we have used for the region close to the vertical asymptota a relation of the form

$$J'_c = \frac{C}{(\gamma_c - a)^s}. \tag{4}$$

The values that best fit the data have been found to be $C=0.38\pm 0.02$, $s=1.07\pm 0.02$, and $a=0.427\pm 0.001$. Notice that the value of this last parameter is in good agreement with previous computations of the critical point of the $S=3/2$ alternating dimerized chain. We stress that Fig. 4 as well as the fits above have been obtained using a fixed finite size; hence, deviations with respect the thermodynamic limit can ocurr. $L=3\times 150$ is, however, a large enough size in these systems, and we expect these possible deviations to affect the precision of our results only to a small extent.

IV. MASSIVE PHASES AND GENERALIZED STRING ORDER PARAMETERS

In this section, we will characterize the quantum phases that appear in the phase diagram in Fig. 4. To achieve this

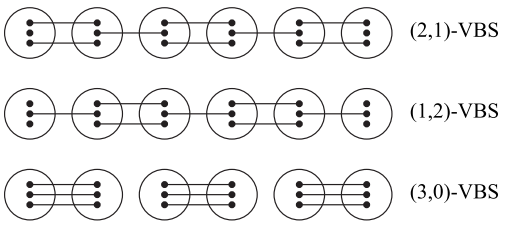

FIG. 5. Valence-bond-solid diagrams of the phases that arise in the models discussed in this paper. Each small solid circle and line represents a spin-1/2 variable and a singlet pair, respectively. The large open circles represent the symmetrization of the spin 1/2 variables on each leg to create a spin-3/2 variable.

goal, we will resort to the generalized string order parameter,[21,24] which are able to detect the VBS state character of dimerized spin systems even when the local spins take on half-integer values. These parameters are generalizations for an arbitrary complex phase of the original string order[23,24] parameter first proposed for the case of integer spin $S=1$. Resorting to the VBS picture (Fig. 5), massive phases corresponding to valence bond solids can be denoted according to the number of valence bonds formed with the contiguous sites; i.e., one particular valence bond solid can be denoted as (m,n)-VBS with $m+n=2S$.

For instance, we have already mentioned in the previous section that in the strong coupling limit, the columnar dimerized three-leg ladder (1) effectively becomes a $S=\frac{3}{2}$ alternating spin chain. Thus, in this case, we have $m+n=3$.

The definition of the generalized string order parameter extended to our particular three-leg ladder with arbitrary size $L=3\times\ell$ is

$$O_{\mathrm{str}}(\theta)=\left|\lim_{j-i\to\infty}\left\langle S^z_{2i}\exp\left(i\theta\sum_{k=2i}^{2j-1}S^z_k\right)S^z_{2j}\right\rangle\right|, \qquad (5)$$

with $0<i<j<\ell/2$ and $S^z_i=S^z_i(1)+S^z_i(2)+S^z_i(3)$. It is actually not necessary to consider $j-i\gg 1$ to obtain accurate values of the parameter, and, typically, a value of $i-j$ of some few tens is enough to give values very close to the infinite limit value, considering that i and j are well within the bulk and far away from the edges. Thereby, for convenience, we will work with the parameter defined as

$$O_{\mathrm{str}}(2i,2j,\ell,\theta)=\left|\left\langle S^z_{2i}\exp\left(i\theta\sum_{k=2i}^{2j-1}S^z_k\right)S^z_{2j}\right\rangle\right|, \qquad (6)$$

with i,j and S^z_i defined as before.

It has been shown[21] that the generalized string order parameter evaluated in $\theta=\pi$ acts as an order parameter since it vanishes or not depending on the number of bonds n being odd or even. Moreover, the shape of the string order parameter in the region $\theta\in[0,2\pi]$ provides us with valuable information about the VBS character of the phases since the number of zeros in this range coincides with the number of bonds m.[21]

Figure 6 shows the parameter O_{str} computed in the completely antiferromagnetic model (2) in the whole range of γ for various values of J'. The operator clearly distinguishes

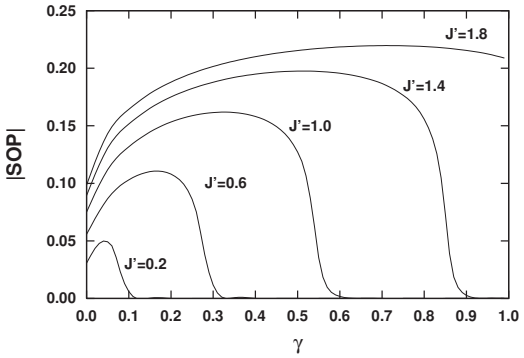

FIG. 6. Generalized string order parameter $O_{\mathrm{str}}(i=20,\ j=42,\ \ell=80,\ \theta=\pi)$ computed in the completely antiferromagnetic model (2) with alternated staggering for several fixed values of J'. Regions where the string order parameter vanishes correspond to a different quantum phase from that where it is non-null. Notice that there exists a certain J' above which the system only exhibits one quantum phase irrespective of the value of γ. This value corresponds to the J' coordinate with $\gamma_c=1$ of the critical line of Fig. 4.

regions where it is finite from others where it vanishes. Moreover, for a fixed value of J', the value of γ where it decays to zero coincides[30] with the critical value γ_c corresponding to that value of J' in the critical line of Fig. 4. On the other hand, Fig. 7 shows O_{str} computed in the ferromagnetic model (1) in the strong coupling regime. For strong values of the ferromagnetic coupling J', we should expect that our ladder behave like an effective $S=3/2$ alternating spin chain. Indeed, we can observe that the string order parameter is clearly nonvanishing above $\gamma=0.42$, the critical point of the chain. As for the region below this point, the tendency of the string order parameter is to decay to zero as we increase the size of the system, except for the point $\gamma=0$ and its vicinity. In fact, this behavior is anomalous since $\gamma=0$ is critical in the chain; therefore, the string order parameter should vanish. In the Appendix, we have addressed this issue with the pure $S=3/2$ alternating dimerized chain. Our study of the chain explains the behavior of the ladder and shows that, indeed, the string order parameter decays to zero also at this point. The decay rate is, however, slower, and it is not enough to increase the size of the ladder. Figure

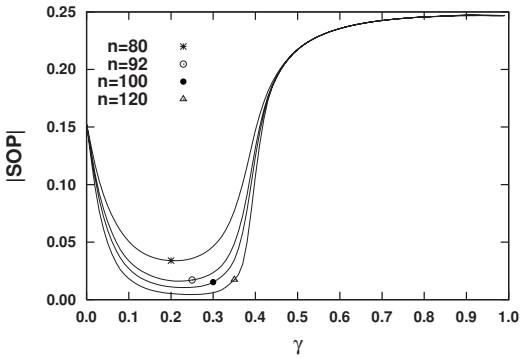

FIG. 7. Generalized string order parameter $O_{\mathrm{str}}(i=\ell/2-24,j=\ell/2+26,\ell=n,\theta=\pi)$ computed in the strong ferromagnetic regime $J'=-25$ of the ferromagnetic model (1) with columnar staggering. See the text for explanations.

9(b) shows that we have to additionally consider sites i and j further and further apart to make the string order parameter decay at $\gamma=0$.

With the considerations explained in the previous paragraph, we have proven that the string order parameter (6) evaluated in $\theta=\pi$ is valid to identify quantum phase transitions in both models (1) and (2). Now, we want to extend the study to the whole θ domain to test the nature of the massive phases. In fact, from definition (6), $O_{\mathrm{str}}(i,j,\ell,\theta)=O_{\mathrm{str}}(i,j,\ell,2\pi-\theta)$; hence, we can restrict the study to the range $\theta\in[0,\pi]$. We will study first the ferromagnetic model (1) with columnar staggering. As we discussed in the previous sections, we can guess the phases of the diagram going to the strong coupling limit $|J'|\gg 1$. In this regime, the ferromagnetic coupling among rungs is the leading interaction and the ladder transforms into an effective $S=3/2$ alternating spin chain. Resorting to continuity arguments, the phases of the ladder must be the same as those that appear in the strong coupling limit, i.e., a (2, 1)-VBS in the region $0<\gamma<\gamma_c$ and a (3, 0)-VBS when $\gamma_c<\gamma\leqslant 1$. In Fig. 8(b), we show O_{str} computed in the θ domain. All the curves appearing in the figure correspond to a fixed $\gamma=0.35$. According to Fig. 4, this value of γ cuts the critical line in a certain value of J', and so we should notice a qualitative change in the curves in Fig. 8. This change can be observed since plots corresponding to very negative J' have a local minimum at $\theta=\pi$, while they change to become a maximum as we move toward J' close to zero. Hence, the number of zeroes in the domain $\theta\in[0,2\pi)$ moves from 1 to 2. In fact, the string order parameter is not strictly equal to zero in our graphs. However, this fact had already been pointed out in spin chains,[28] and it had been conclusively proven that it was due to finite-size effects. The values closer to zero are attained considering larger sizes. According then to the VBS notation and our DMRG results, we can label the phases of model (1) as (2, 1)-VBS in the region $0<\gamma<\gamma_c$ and (3, 0)-VBS for $\gamma_c<\gamma\leqslant 1$, as expected from the knowledge of the $S=3/2$ chain.

The completely antiferromagnetic model has more difficulty guessing *a priori* the quantum phases that arise or if their ground states are valence bond solids. We have used again the generalized string order parameters to check the nature of the phases. Figure 8(a) shows the string order parameter as a function of θ and a fixed value $\gamma=0.5$, which cuts the critical line. It can be seen that, indeed, the SOP behaves as expected for a VBS state, and two phases can be identified attending to the number of zeros in this domain. For higher values of J', the SOP has a maximum at $\theta=\pi$ and only one zero in the region $0\leqslant\theta<2\pi$. As we consider lower values of J', more precisely in the interval from $J'=1.0$ to $J'=0.8$, the SOP at $\theta=\pi$ falls abruptly to zero; therefore, the SOP has two vanishing values in the aforementioned interval. From these results, we can conclude, first, that both massive phases can be properly described as valence bond solids and they can also be identified as a (1, 2)-VBS for $0\leqslant\gamma<\gamma_c$ and a (2, 1)-VBS for $\gamma_c<\gamma\leqslant 1$.

V. CONCLUSIONS

We have given a precise meaning to the conjectured phase diagrams[11] corresponding to three-leg Heisenberg ladders with columnar dimerization and ferromagnetic rung couplings on one side and, similarly, to that with alternating dimerization and antiferromagnetic couplings among the rungs. Although both models exhibit critical lines, their qualitative form is different: In the former, the critical line approaches an asymptota at the critical value $\gamma_c=0.42$ where it effectively becomes an alternating $S=\frac{3}{2}$ spin ladder. On the contrary, the latter model does not exhibit any asymptota, but the critical line meets the wall $\gamma=1$ of the phase diagram.

Moreover, we have also clarified the valence-bond-solid nature of the massive phases separated by the critical lines in the phase diagram. In this regard, we have found that the generalized string order parameters are a very good tool for characterizing VBS state phases in ladders with a variety of dimerization patterns. Our results are based on extensive calculations using the finite-size DMRG technique.

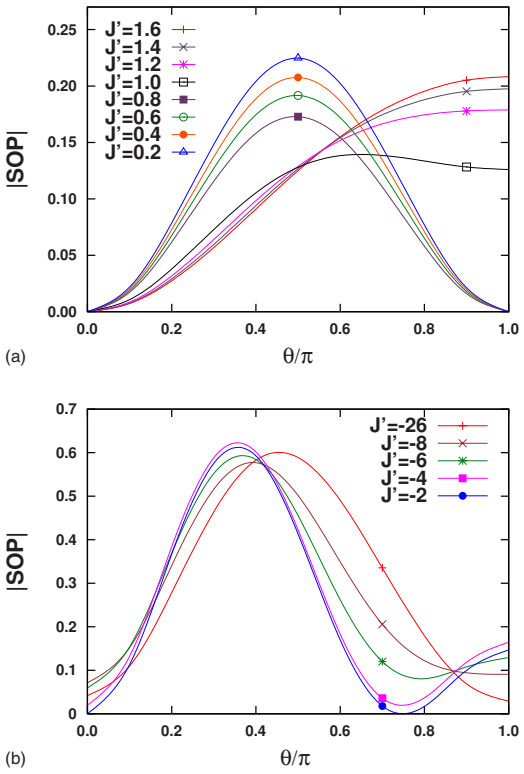

FIG. 8. (Color online) Generalized string order parameter $O_{\mathrm{str}}(i=20,j=42,\ell=80,\theta)$ computed in (a) the completely antiferromagnetic model at $\gamma=0.5$ and (b) the ferromagnetic model at $\gamma=0.35$. According to Fig. 4, these values cut the critical lines at ($\gamma_c=0.5$, $J'_c=0.96$) and ($\gamma_c=0.35$, $J'_c=-6.1$), respectively. It can be observed that both graphs show a change in the number of zeros near these points.

ACKNOWLEDGMENTS

Part of the computations of this work were performed with the High Capacity Computational Cluster for Physics of UCM (HC3PHYS UCM), funded in part by UCM and in part by FEDER funds. We acknowledge financial support from DGS grants under Contracts No. BFM 2003-05316-C02-01 and No. FIS2006-04885 and from the ESF Science Pro-

gramme INSTANS 2005-2010.

APPENDIX: THE $S=3/2$ STAGGERED SPIN CHAIN

It was already pointed out by Oshikawa[21] that half-integer systems are amenable to have many order parameters. We want to compare in this section two order parameters that—despite differing only slightly in their definition—have, in fact, quite different behaviors and may even lead to confusion. We will see that both parameters capture the quantum phase transition of the chain, but only one can go further and give evidences of the quantum phases themselves.

The string order parameters are defined as

$$O_{\mathrm{str}}^{\mathrm{even}}(\theta,L)=\left|\lim_{j-i\to\infty}\left\langle S_{2i}^{z}\exp\left(i\theta\sum_{\ell=2i}^{2j-1}S_{\ell}^{z}\right)S_{2j}^{z}\right\rangle\right|, \quad \text{(A1)}$$

with $0<i<j\leqslant L/2$, and

$$O_{\mathrm{str}}^{\mathrm{odd}}(\theta,L)=\left|\lim_{j-i\to\infty}\left\langle S_{2i+1}^{z}\exp\left(i\theta\sum_{\ell=2i+1}^{2j}S_{\ell}^{z}\right)S_{2j+1}^{z}\right\rangle\right|, \quad \text{(A2)}$$

with $0\leqslant i<j<L/2$.

Notice that, including the edges, both definitions involve an odd number of spins between sites $2i$ and $2j$ or $2i+1$ and $2j+1$ and an even number of antisymmetric operators under spin flip. This condition is required to obtain a value of the mean value different from zero.

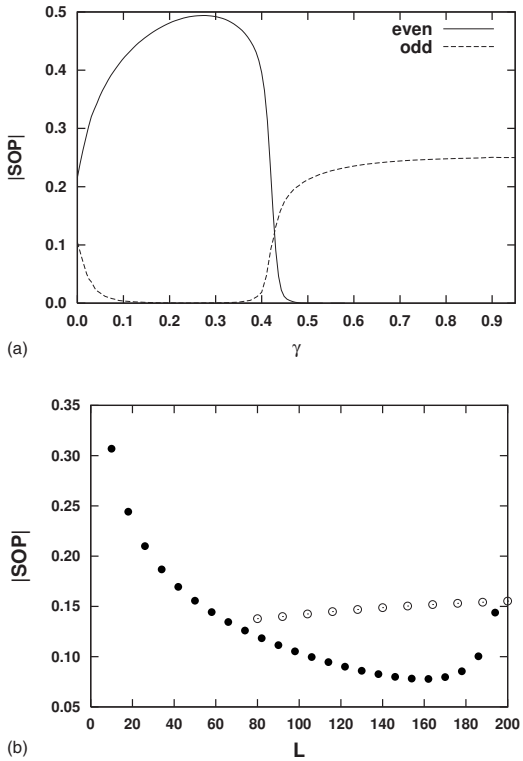

FIG. 9. (a) String order parameters $O_{\mathrm{str}}^{\mathrm{odd}}(i=51,j=131,L=180,\theta=\pi)$ (solid line) and $O_{\mathrm{str}}^{\mathrm{even}}(i=52,j=130,L=180,\theta=\pi)$ (dashed line) computed in a $S=3/2$ alternating dimerized chain. (b) String order parameter $O_{\mathrm{str}}^{\mathrm{even}}$ at $\gamma=0$ varying the total length of the chain $O_{\mathrm{str}}^{\mathrm{even}}(i=N/2-24,j=N/2+26,L=N,\theta=\pi)$ (empty circles) and varying the distance $i-j$, $O_{\mathrm{str}}^{\mathrm{even}}(i=(L-N+1)/2+1,j=i+N-1,L=200,\theta=\pi)$ (solid circles).

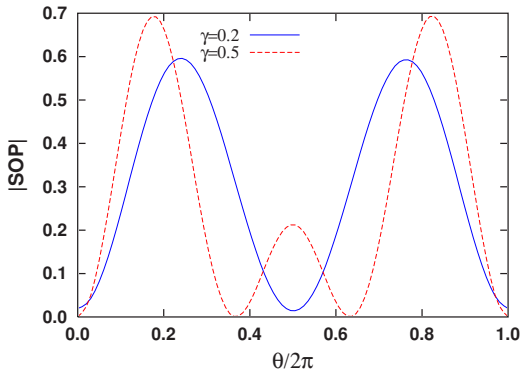

FIG. 10. (Color online) string order parameter $O_{\mathrm{str}}^{\mathrm{even}}(i=22,j=80,L=100,\theta)$ computed below and above the critical point $\gamma_c=0.42$ of a $S=3/2$ alternating dimerized chain. The number of zeros of this parameter determines the nature of the valence bond solid at each phase.

It has been commented in the previous sections that the $S=3/2$ alternating dimerized chain has three critical points at $\gamma_c=0$ and $\gamma_c=\pm 0.42$ in the interval $\gamma\in[-1,1]$. The phase diagram is symmetric with respect to $\gamma=0$. Therefore, we can constrain our study to the region $0\leqslant\gamma$.

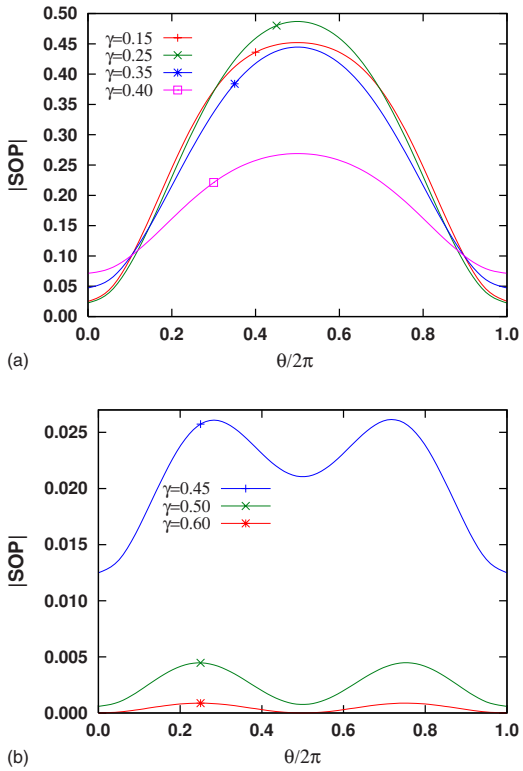

FIG. 11. (Color online) string order parameter $O_{\mathrm{str}}^{\mathrm{odd}}(i=21,j=79,L=100,\theta)$: (a)computed below the critical point and (b) computed above the critical point $\gamma_c=0.42$ of a $S=3/2$ alternating dimerized chain. In this latter case, the string order parameter in the θ does not clearly determine the valence bond phases of the chain. Notice also the appreciable change of scale from one phase to the other.

As regards the interval $0<\gamma<\gamma_c$, the ground state is known to be a (2, 1)-VBS, while for $\gamma_c<\gamma\leqslant 1$, it is a (3, 0)-VBS. The first issue we have to check is wether or not the parameters defined above can make explicit this quantum phase transition. In Fig. 9(a), we have plotted both parameters $O_{\mathrm{str}}^{\mathrm{odd}}(\pi,L)$ and $O_{\mathrm{str}}^{\mathrm{even}}(\pi,L)$ in the range $0\leqslant\gamma\leqslant 1$. This graph shows that both operators are finite at one side of the critical point, while thay vanish at the other (Figs. 10 and 11). We can conclude then that they act as proper order parameters in the phase transition. However, a clear major difference can be noticed from this figure since each one of these order parameters, in fact, vanishes on differents sides of the critical point.

[1] F. D. M. Haldane, Phys. Lett. **93A**, 464 (1982).
[2] E. Dagotto and T. M. Rice, Science **271**, 618 (1996).
[3] *Strongly Correlated Magnetic and Superconducting Systems*, Lecture Notes in Physics, Proceedings of the El Escorial Summer School 1996, edited by G. Sierra and M. A. Martin-Delgado (Springer-Verlag, New York, 1997).
[4] E. Dagotto, Rep. Prog. Phys. **62**, 1525 (1999).
[5] Z. Hiroi, M. Azuma, M. Takano, and Y. Bando, J. Solid State Chem. **95**, 230 (1991).
[6] M. Azuma, Z. Hiroi, M. Takano, K. Ishida, and Y. Kitaoka, Phys. Rev. Lett. **73**, 3463 (1994).
[7] B. Batlogg *et al.*, Bull. Am. Phys. Soc. **40**, 327 (1995).
[8] Y. Hosokoshi, Y. Nakazawa, K. Inoue, K. Takizawa, H. Nakano M. Takahashi, and T. Goto, Phys. Rev. B **60**, 12924 (1999).
[9] M. Greiner, O. Mandel, T. Esslinger, Th. W. Hänsch, and I. Bloch, Nature (London) **415**, 39 (2002); M. Greiner, O. Mandel, Th. W. Hänsch, and I. Bloch, *ibid.* **419**, 51 (2002).
[10] J. J. Garcia-Ripoll, M. A. Martin-Delgado, and J. I. Cirac, Phys. Rev. Lett. **93**, 250405 (2004).
[11] M. A. Martin-Delgado, R. Shankar, and G. Sierra, Phys. Rev. Lett. **77**, 3443 (1996).
[12] V. N. Kotov, J. Oitmaa, and Zheng Weihong, Phys. Rev. B **59**, 11377 (1999).
[13] Y.-J. Wang and A. A. Nersesyan, Nucl. Phys. B **583**, 671 (2000).
[14] M. A. Martín-Delgado, J. Dukelsky, and G. Sierra, Phys. Lett. A **250**, 87 (1998).
[15] K. Okamoto, Phys. Rev. B **67**, 212408 (2003).
[16] S. R. White, Phys. Rev. Lett. **69**, 2863 (1992).
[17] S. R. White, Phys. Rev. B **48**, 10345 (1993).
[18] K. Hallberg, Adv. Phys. **55**, 477 (2006).
[19] A. Schollwöck, Rev. Mod. Phys. **77**, 259 (2005).
[20] *Density Matrix Renormalization*, Lecture Notes in Physics, edited by I. Peschel, X. Wang, M. Kaulke, and K. Hallberg (Springer, Berlin, 1999).
[21] M. Oshikawa, J. Phys.: Condens. Matter **4**, 7469 (1992).
[22] I. Affleck and F. D. M. Haldane, Phys. Rev. B **36**, 5291 (1987).
[23] M. den Nijs and K. Rommelse, Phys. Rev. B **40**, 4709 (1989).
[24] T. Kennedy and H. Tasaki, Phys. Rev. B **45**, 304 (1992).
[25] J. Almeida, M. A. Martin-Delgado, and G. Sierra, Phys. Rev. B **76**, 184428 (2007).
[26] I. Affleck, *Fields, Strings and Critical Phenomena*, Les Houches 1988-Session XLIX (North-Holland, Amsterdam, 1990), Chap. 10, pp. 563–640.
[27] M. Yajima and T. Takahashi, J. Phys. Soc. Jpn. **65**, 39 (1996).
[28] S. Yamamoto, Phys. Rev. B **55**, 3603 (1997).
[29] T. Kennedy, J. Phys.: Condens. Matter **2**, 5737 (1990).
[30] With less precision since computations in Fig. 6 were performed in shorter ladders.